Correspondence

The Effective Throughput of MISO Systems Over κ–μ Fading Channels

Jiayi Zhang, *Student Member, IEEE*, Zhenhui Tan, Haibo Wang, Qing Huang, and Lajos Hanzo, *Fellow, IEEE*

***Abstract*—The *effective throughput* of multiple-input–single-output (MISO) systems communicating over both independent and identically distributed (i.i.d.) and independent and nonidentically distributed (i.n.i.d.) κ–μ fading channels is investigated under delay constraints. New analytical expressions are derived for the exact effective throughput of both channels. Moreover, we present tractable closed-form effective throughput expressions in the asymptotically high- and low-signal-to-noise-ratio (SNR) regimes for i.i.d. κ–μ fading channels. These results enable us to investigate the impact of system parameters on the effective throughput of MISO κ–μ fading channels. We demonstrate that as the affordable delay tends to infinity, the effective throughput is increased to the classic ergodic capacity. By contrast, the effective throughput of delay-constrained near-real-time systems fails to approach the ergodic capacity.**

***Index Terms*—Delay constraint, delay-limited capacity, effective capacity, κ–μ distribution, multiple-input single-output (MISO).**

I. Introduction

The ergodic capacity of multiple-antenna systems has been investigated for transmission over various fading channels in [1]–[3]. However, emerging real-time applications, such as voice over Internet Protocol and mobile TV, have imposed stringent quality-of-service (QoS) constraints. **In this context, Shannon's ergodic capacity cannot account for the transmission delay of the system. However, it would be highly desirable to quantify the delay-limited capacity of a system, which is a challenging task. The first contribution in this content was produced by Hanly and Tse in** [4]. Hence, a QoS metric capable of capturing the delay constraints of communication systems is required. Motivated by this open problem, the concept of effective throughput (or effective capacity, effective rate) has been proposed in [5] for taking the system's delay into account. Since then, several authors have investigated the effective capacity of various systems. For example, Femenias *et al.* in [6] investigated the effective capacity of wireless cross-layer networks combining adaptive modulation and coding at the physical layer with an automatic repeat request protocol at the data-link layer. In [7], an analytical model of the effective capacity found in proportional fair scheduling used in orthogonal frequency-division multiple-access systems in the context of user multiplexing was presented.

The effective throughput of multiple-input–single-output (MISO) systems, such as the optimal precoding scheme relying on covariance feedback, was derived for correlated MISO systems [8], whereas that of correlated MISO channels was presented in [9]. In [10], Li characterized the effective throughput of cognitive MISO systems subjected to channel estimation errors. Moreover, Matthaiou *et al.* in [11] provided a detailed effective throughput analysis of Nakagami-m, Rician, and generalized-K MISO fading channels. However, the existence of these well-known fading distributions is based on the assumption of a homogeneous scattering environment, which is often unrealistic, since the waves reflected by a surface are spatially correlated in most propagation environments.

Hence, the κ–μ distribution has been proposed in [12] for characterizing the inhomogeneous nature of fading channels. This generalized fading model is capable of providing a better fit to experimental data than the aforementioned models. Additionally, it has been shown in [12] that the κ–μ distribution encompasses the Rician, Nakagami-m, and Rayleigh distributions as special cases. *Against this background, we solve the open problem of providing both exact and asymptotic high-signal-to-noise-ratio (SNR) and low-SNR expressions for the effective throughput of independent and identically distributed (i.i.d.) and independent and nonidentically distributed (i.n.i.d.) κ–μ fading channels.*

The rest of this paper is organized as follows. Section II describes the general system model and the mathematical characteristics of κ–μ fading channels. In Section III, we derive new exact expressions for the effective throughput of MISO systems communicating over i.i.d. κ–μ fading channels and present closed-form effective throughput expressions both for high SNRs and for the minimum transmit energy per information bit for the sake of quantifying the effect of system parameters on the effective throughput. Moreover, the effective throughput for the case of i.n.i.d. κ–μ fading channels is analyzed in Section IV. Finally, our theoretical and Monte Carlo simulation results are compared in Section V in terms of the effective throughput, and Section VI concludes this paper.

II. System and Channel Model

We consider a MISO system model and assume that the transmitter is equipped with N_t antennas. The flat-fading channel's input–output relation can be expressed as $y = \mathbf{h}\mathbf{x} + n$, where $\mathbf{h} \in \mathbb{C}^{1\times N_t}$ denotes the MISO channel's fading vector, whereas $\mathbf{x}$ is the transmit vector having a covariance of $\mathtt{E}\{\mathbf{x}\mathbf{x}^\dagger\} = \mathbf{Q}$, where $\mathtt{E}\{\cdot\}$ is the expectation operator, which is subjected to the sum-power constraint of $\mathrm{tr}(\mathbf{Q}) \le P$, where $\mathrm{tr}(\cdot)$ is the matrix trace. Moreover, n represents the complex additive white Gaussian noise term with zero mean and variance N_0, respectively. Finally, we assume that the same power is assigned to the transmit antennas; hence, we have $\mathbf{Q} = (P/N_t)\mathbf{I}$.

As a generalized link-level capacity notion of uncorrelated stationary fading channels, whose response varies from one transmission block to another by obeying a certain distribution but remains constant

Manuscript received January 2, 2013; revised August 5, 2013; accepted August 6, 2013. This work was supported in part by the National Natural Science Foundation of China under Grant 61071075 and Grant 61001071, by the National ST Major Project under Grant 2011ZX03005-004-03, and by the Fundamental Research Funds for the Central Universities under Grant 2012JBM018. The review of this paper was coordinated by Prof. M. Daoud.

J. Zhang is with the Institute of Broadband Wireless Mobile Communications and the State Key Laboratory of Rail Traffic Control and Safety, Beijing Jiaotong University, Beijing 100044, China (e-mail: jayizhang@bjtu.edu.cn).

Z. Tan, H. Wang, and Q. Huang are with the Institute of Broadband Wireless Mobile Communications, Beijing Jiaotong University, Beijing 100044, China (e-mail: zhhtan@bjtu.edu.cn; hbwang@bjtu.edu.cn; qhuang1@bjtu.edu.cn).

L. Hanzo is with the School of Electrical and Computer Science, University of Southampton, Southampton SO17 1BJ, U.K. (e-mail: lh@ecs.soton.ac.uk).

Color versions of one or more of the figures in this paper are available online at http://ieeexplore.ieee.org.

Digital Object Identifier 10.1109/TVT.2013.2277992

within a single block, the effective capacity of the service process is defined as [13][1]

$$\alpha(\theta) = -(1/\theta T)\, \ln\left(\mathtt{E}\left\{\exp(-\theta T C)\right\}\right), \qquad \theta \neq 0 \tag{1}$$

where C represents the system's throughput during a single block, and T denotes the duration of the block, whereas the delay exponent

$$\theta = -\lim_{l_{\rm th}\to\infty} \frac{\ln \Pr[L > l_{\rm th}]}{l_{\rm th}} \tag{2}$$

of (1) reflects that any throughput improvement attained at the cost of a high delay is devalued. In (2), $l_{\rm th}$ is the threshold of queue length, and L is the equilibrium queue length of the buffer assumed to be available at the transmitter. When $l_{\rm th} \to \infty$, the tail distribution function $\Pr[L > l_{\rm th}]$ can be asymptotically written as $\Pr[L > l_{\rm th}] \approx e^{\theta l_{\rm th}}$ according to the large deviations theory [5]. Again, the delay exponent has to satisfy the constraint of $\theta \geq \theta_0$, where θ_0 is the minimum required decay rate. Once a delay requirement is violated, the corresponding data packet is discarded in the queue. More particularly, a larger θ_0 implies a tighter delay constraint. Note that when no delay constraint is imposed, i.e., we have $\theta_0 \to 0$, the effective throughput tends to the classic ergodic throughput of the corresponding wireless channel.

Assuming that the transmitter sends uncorrelated circularly symmetric zero-mean complex Gaussian signals, the effective throughput can be succinctly expressed as follows [11]:

$$R(\rho,\theta) = -\frac{1}{A}\log_2\left(\mathtt{E}\left\{\left(1+\frac{\rho}{N_t}\mathbf{h}\mathbf{h}^{\dagger}\right)^{-A}\right\}\right) \ \text{bits/s/Hz} \tag{3}$$

where we have $A = \theta T B/\ln 2$, with B denoting the bandwidth of the system, whereas ρ is the average SNR.

The κ–μ distribution models the small-scale variation of the fading signal in a nonhomogeneous environment. The probability density function (pdf) of the κ–μ fading channels' output SNR is given by [12, eq. (10)]

$$p_{\kappa-\mu}(\omega) = \frac{\mu(1+\kappa)^{\frac{\mu+1}{2}}\omega^{\frac{\mu-1}{2}}}{\exp(\mu\kappa)\kappa^{\frac{\mu-1}{2}}\Omega^{\frac{\mu+1}{2}}}\exp\left(-\frac{\mu(1+\kappa)\omega}{\Omega}\right) \times I_{\mu-1}\left(2\mu\sqrt{\frac{\kappa(1+\kappa)\,\omega}{\Omega}}\right) \tag{4}$$

where κ denotes the ratio between the total power of the dominant components and the total power of the scattered waves, μ is related to the number of multipath clusters, and $I_v(\cdot)$ is the modified Bessel function of the first kind with order v [14, eq. (8.445)].

III. Independent and Identical κ–μ Fading

A. Exact Analysis

Here, we present the exact effective throughput analysis of the κ–μ fading models introduced in Section II. More specifically, the entries of channel vector $\mathbf{h}$ are assumed to be i.i.d. κ–μ random variables (RVs).

We commence our analysis by invoking [12], where it was shown that the sum of M i.i.d. squared κ–μ distributed RVs with parameters κ, μ, and Ω is also a κ–μ distribution with parameters κ, $M\mu$, and $M\Omega$. Using [12, eq. (10)], after a number of manipulations, we arrive at the pdf of $z = \sum_{k=1}^{N_t}|h_k|^2$, i.e.,

$$p_{\text{i.i.d.}}(z) = \frac{\mu N_t(1+\kappa)^{\frac{\mu N_t+1}{2}} z^{\frac{\mu N_t-1}{2}}}{e^{\mu N_t\kappa}\kappa^{\frac{\mu N_t-1}{2}}(\Omega N_t)^{\frac{\mu N_t+1}{2}}}\exp\left(-\frac{\mu(1+\kappa)z}{\Omega}\right) \times I_{\mu N_t-1}\left(2u\sqrt{\frac{\kappa(1+\kappa)N_t z}{\Omega}}\right) \tag{5}$$

$$= \frac{\mu N_t(1+\kappa)^{\frac{\mu N_t+1}{2}} z^{\frac{\mu N_t-1}{2}}}{e^{\mu N_t\kappa}\kappa^{\frac{\mu N_t-1}{2}}(\Omega N_t)^{\frac{\mu N_t+1}{2}}}\exp\left(-\frac{\mu(1+\kappa)z}{\Omega}\right) \times \sum_{l=0}^{\infty}\frac{1}{l!\Gamma(\mu N_t+l)}\left(\mu\sqrt{\frac{\kappa(1+\kappa)N_t z}{\Omega}}\right)^{\mu N_t+2l-1} \tag{6}$$

where we proceed from (5) to (6) by exploiting [14, eq. (8.445)]. Upon substituting (6) into (3), there is an integral in the form of $(1+\rho z/N_t)^{-A}$, $z^{\mu N_t+l-1}$, and $\exp(-(\mu(1+\kappa)z/\Omega))$. The effective throughput of MISO i.i.d. κ–μ fading channels is given by

$$R_{\text{i.i.d.}}(\rho,\theta) = \frac{\mu N_t\kappa}{A\ln 2} + \log_2\left(\frac{\Omega\rho}{\mu N_t(1+\kappa)}\right) - \frac{1}{A}\log_2\left(\sum_{l=0}^{\infty}\frac{(\mu N_t\kappa)^l}{\Gamma(l+1)}U\left(A; A+1-\mu N_t-l; \frac{\mu N_t(1+\kappa)}{\Omega\rho}\right)\right) \tag{7}$$

where $U(\cdot)$ is the Tricomi hypergeometric function [14, eq. (13.1.3)], and we have used the integral equation of [15, eq. (39)], i.e.,

$$\int_0^{\infty}(1+ax)^{-v}x^{q-1}e^{-px}dx = a^{-q}\Gamma(q)U\left(q, q+1-v, p/a\right)$$

where the conditions of $\mathrm{Re}(q) > 0$, $\mathrm{Re}(p) > 0$, and $\mathrm{Re}(a) > 0$ are met. In addition, Kummer's transformation $U(a;b;x) = x^{1-b}U(a-b+1; 2-b; x)$ [16, eq. (07.33.17.0007.01)] is used. Note that for the case of Rician fading channels (e.g., $\kappa = K$, $\mu = 1$, where K is the Rician K-factor), (7) reduces to [11, eq. (34)].

Since (7) is expressed in the form of an infinite series, we should demonstrate its convergence by seeking to quantify the truncation error imposed by a limited number of terms. Assuming that T_0 terms are used, the associated truncation error E_0 can be expressed as

$$E_0 = \sum_{l=T_0}^{\infty}\frac{(\mu N_t\kappa)^l}{\Gamma(l+1)}U\left(A; A+1-\mu N_t-l; \frac{\mu N_t(1+\kappa)}{\Omega\rho}\right) < U\left(A; A+1-\mu N_t-T_0; \frac{\mu N_t(1+\kappa)}{\Omega\rho}\right)\sum_{l=T_0}^{\infty}\frac{(\mu N_t\kappa)^l}{\Gamma(l+1)} \tag{8}$$

where we have exploited the fact that $U(a, b-l, z)$ is a monotonically decreasing function of l. With the aid of [17, eq. (6.5.4)] and [17, eq. (6.5.29)], (8) may be streamlined to

$$E_0 < U\left(A; A+1-\mu N_t-T_0; \frac{\mu N_t(1+\kappa)}{\Omega\rho}\right) \times \exp\left(\mu\kappa N_t\right)\left(1-\frac{\Gamma(T_0,\mu\kappa N_t)}{\Gamma(T_0)}\right) \tag{9}$$

where $\Gamma(\cdot,\cdot)$ represents the upper incomplete gamma function [14, eq. (8.350.2)].

[1]The packet arrival process and the server strategy employed in the queuing system are those introduced in [5] and [13].

The given expressions are exact; however, they only provide limited physical insights into the quantitative effects of the parameters (e.g., the number of transmit antennas, the delay-related exponent, and the number of multipath clusters) on the effective throughput. Let us hence elaborate further by considering both the high- and low-SNR regions of operation.

B. Asymptotic Analysis

We commence with the high-SNR analysis. By retaining only the dominant term in (3) as $\rho \to \infty$, we arrive at

$$\mathtt{E}\left\{\left(\frac{\rho}{N_t}\mathbf{h}\mathbf{h}^\dagger\right)^{-A}\right\} = \left(\frac{\rho}{N_t}\right)^{-A} \frac{\mu N_t (1+\kappa)^{\frac{\mu N_t+1}{2}}}{e^{\mu N_t \kappa}\kappa^{\frac{\mu N_t-1}{2}}(\Omega N_t)^{\frac{\mu N_t+1}{2}}} \times \int_0^\infty \frac{z^{(\mu N_t-1)/2-A}}{\exp\left(\mu(1+\kappa)\,z/\Omega\right)} I_{\mu N_t-1}\left(2\mu\sqrt{\frac{\kappa(1+\kappa)\,N_t z}{\Omega}}\right) dz. \tag{10}$$

The given integral can now be evaluated using [18, eq. (3.15.2.5)], upon exploiting that $A < \mu N_t$. Finally, the effective throughput attained at high SNRs and for $A < \mu N_t$ may be approximated for MISO κ–μ fading channels as

$$R^{\infty}_{\text{i.i.d.}}(\rho,\theta) = \log_2\left(\frac{\Omega\rho}{\mu N_t(1+\kappa)}\right) + \frac{\kappa\mu N_t}{A\ln 2} - \frac{1}{A}\log_2\left(\frac{\Gamma(\mu N_t - A)}{\Gamma(\mu N_t)}\,{}_1F_1(\mu N_t - A;\mu N_t;\kappa\mu N_t)\right) \tag{11}$$

where ${}_1F_1$ is the confluent hypergeometric function [14, eq. (9.238.2)]. Note that the effective throughput achieved at high SNRs is a monotonically increasing function of κ. This is anticipated, since larger values of κ result in more deterministic fading. When considering the Rician fading case, (11) reduces to [11, eq. (49)].

Let us now investigate the effective throughput of κ–μ fading channels in the power-limited low-SNR region, where the effective throughput can be approximated by a second-order Taylor expansion of the SNR following the generic methodology in [19]. More particularly, we can approximate the effective throughput as $\rho \to 0^+$ according to

$$R(\rho,\theta) = R'(0,\theta)\,\rho + R''(0,\theta)\frac{\rho^2}{2} + o\left(\rho^2\right) \tag{12}$$

where $R'(0,\theta)$ and $R''(0,\theta)$ denote the first- and second-order derivatives of the effective throughput with respect to the SNR, ρ, at $\rho = 0$, respectively.

However, it has been shown in [20] that the Taylor expansion method may, in fact, result in misleading conclusions regarding the impact of the channel in the low-SNR region. Hence, it is beneficial to explore the effective throughput at low SNRs in terms of the normalized transmit energy per information bit E_b/N_0, which is formulated as [20]

$$R\left(\frac{E_b}{N_0}\right) \approx S_0 \log_2\left(\frac{E_b}{N_0} \Big/ \frac{E_b}{N_0}_{\min}\right) \tag{13}$$

where $E_b/N_{0\min}$ is the minimum normalized energy per information bit required for reliably conveying any nonzero throughput, whereas S_0 denotes the throughput versus SNR slope defined in [8]. These metrics are defined respectively as

$$\frac{E_b}{N_0}_{\min} \triangleq \lim_{\rho\to 0}\frac{\rho}{R(\rho,\theta)} = \frac{1}{R'(0,\theta)} \tag{14}$$

$$S_0 \triangleq -\frac{2\left[R'(0,\theta)\right]^2 \ln 2}{R''(0,\theta)}. \tag{15}$$

Due to space limitations, we omit the explicit details, and upon following a similar line of reasoning as in [9, Appendix I], we arrive at the first- and second-order derivatives seen in (14) and (15) in the form of

$$R'(0,\theta) = \frac{1}{N_t \ln 2}\mathtt{E}\{\mathbf{h}\mathbf{h}^\dagger\} \tag{16}$$

$$R''(0,\theta) = \frac{A}{N_t^2 \ln 2}\left(\mathtt{E}\{\mathbf{h}\mathbf{h}^\dagger\}\right)^2 - \frac{A+1}{N_t^2\ln 2}E\left\{(\mathbf{h}\mathbf{h}^\dagger)^2\right\}. \tag{17}$$

Recalling that $\mathtt{E}\{|h_k|^2\} = \Omega$, we may readily infer that $\mathtt{E}\{\mathbf{h}\mathbf{h}^\dagger\} = N_t\Omega$. With the aid of (4) and [18, eq. (3.15.2.5)], the fourth moment of $|h_k|$ can now be expressed as

$$\mathtt{E}\left\{|h_k|^4\right\} = N_t\Omega^2\left(\frac{1+2\kappa}{\mu(1+\kappa)^2} + N_t\right) \tag{18}$$

where we have utilized [14, eq. (9.212.1)] and [14, eq. (9.210.1)]. With (18) at our disposal, we can readily deduce that

$$\begin{aligned}\mathtt{E}\left\{(\mathbf{h}\mathbf{h}^\dagger)^2\right\} &= \mathtt{E}\left\{\left(\sum_{k=1}^{N_t}|h_k|^2\right)^2\right\}\\ &= \sum_{k=1}^{N_t}\mathtt{E}\left\{|h_k|^4\right\} + \sum_{k=1}^{N_t}\sum_{j=1,j\neq k}^{N_t}\mathtt{E}\left\{|h_k|^2|h_j|^2\right\}\\ &= N_t\Omega^2\left(\frac{1+2\kappa}{\mu(1+\kappa)^2} + N_t\right).\end{aligned} \tag{19}$$

Substituting (19) into (17) and then applying (14) and (15), the low-SNR metrics of MISO κ–μ fading channels can be respectively expressed as

$$\frac{E_b}{N_0}_{\min} = \frac{\ln 2}{\Omega} \tag{20}$$

$$S_0 = \frac{2\mu N_t(1+\kappa)^2}{(A+1)(1+2\kappa) + \mu N_t(1+\kappa)^2}. \tag{21}$$

Observe in (21) that the low-SNR slope is an increasing function of both κ and μ, whereas it is a monotonically decreasing function of A, satisfying $0 < S_0 < 2$ for a fixed N_t. It is also worth mentioning that $E_b/N_{0\min}$ is independent of both κ and delay constraint θ. Note that for the case of Rician fading channels, the throughput-versus-SNR-slope expression of (21) reduces to

$$S_0 = \frac{2N_t(K+1)^2}{N_t(K+1)^2 + (A+1)^{2K+1}} \tag{22}$$

which coincides with [11, eq. (41)].

IV. Independent and Nonidentical κ–μ Fading

Let us now move on to consider the case of wireless systems communicating over i.n.i.d. MISO κ–μ fading channels. The pdf of the sum of M i.n.i.d. squared κ–μ distributed RVs associated with parameters κ_m, μ_m, and Ω_m is given by [21, eq. (4)], i.e.,

$$p_{\text{i.n.i.d.}}(z) = \frac{e^{-\frac{z}{2\beta}} z^{V-1}}{(2\beta)^V \Gamma(V)} \sum_{k=0}^{\infty} \frac{k! c_k}{(V)_k} L_k^{(V-1)}\left(\frac{Uz}{2\beta\xi}\right) \tag{23}$$

where $V = \sum_{m=1}^{M} \mu_m$, $(u)_v = \Gamma(u+v)/\Gamma(u)$ is the Pochhammer symbol [14], and $L_n^{\alpha}(\cdot)$ is the generalized Laguerre polynomial [16, eq. (05.08.02.0001.01)], namely

$$L_n^v(y) = \frac{\Gamma(v+n+1)}{n!} \sum_{q=0}^{n} \frac{(-n)_q y^q}{q!\Gamma(v+q+1)}, \; n \in \mathbb{N}. \tag{24}$$

Then, (23) can be alternatively expressed as

$$p_{\text{i.n.i.d.}}(z) = \frac{e^{\frac{-z}{2\beta}}}{(2\beta)^V} \sum_{k=0}^{\infty} c_k \sum_{q=0}^{k} \frac{(-k)_q z^{q+V-1}}{q!\Gamma(V+q)} \left(\frac{V}{2\beta\xi}\right)^q. \tag{25}$$

Note that the coefficients c_k can be recursively obtained following the equations [21, eq. (5a–5c)]

$$c_k = \frac{1}{k} \sum_{j=0}^{k} c_j d_{k-j}, \qquad k \geqslant 1 \tag{26}$$

$$c_0 = \left(\frac{V}{\xi}\right)^V \exp\left(-\frac{1}{2} \sum_{m=1}^{M} \frac{\lambda_m a_m (V-\xi)}{\beta\xi + a_m(V-\xi)}\right) \times \prod_{m=1}^{M} \left(1 + \frac{a_m}{\beta}(V/\xi - 1)\right)^{-\mu_m} \tag{27}$$

$$d_j = -\frac{j\beta V}{2\xi} \sum_{m=1}^{M} \lambda_m a_m (\beta - a_m)^{j-1} \left(\frac{\xi}{\beta\xi + a_m(V-\xi)}\right)^{j+1} + \sum_{m=1}^{M} \mu_m \left(\frac{1 - a_m/\beta}{1 + (a_m/\beta)(V/\xi - 1)}\right)^j, \qquad j \geqslant 1 \tag{28}$$

where $\lambda_m = 2\mu_m\kappa_m$, $a_m = \Omega_m / 2\mu_m(1+\kappa_m)$. Note that parameters ξ and β are chosen to guarantee the uniform convergence of (23) according to [22, Remark 3.1]. By substituting (25) into (3) and using the identity [15, eq. (39)], we arrive at the effective throughput expression of MISO i.n.i.d. κ–μ fading channels formulated as

$$R_{\text{i.n.i.d.}} = \log_2\left(\frac{2\beta\rho}{N_t}\right) - \frac{1}{A} \sum_{k=0}^{\infty} c_k \sum_{q=0}^{k} \frac{(-k)_q}{q!} \left(\frac{V}{\xi}\right)^q \times U\left(A; A+1-q-V; \frac{N_t}{2\beta\rho}\right). \tag{29}$$

V. Numerical Results

Here, the theoretical analysis presented in Sections III and IV is validated with the aid of Monte Carlo simulations, which were derived by averaging the results over 10^7 independent κ–μ channel realizations. We generate the squared κ–μ fading samples using the noncentral chi-square distribution method in [21]. These results are provided for characterizing the effects of different system and channel parameters on the effective throughput of MISO systems communicating over κ–μ fading channels. Without loss of generality, we normalize the bandwidth of the system as $B = 1$ Hz.

In Fig. 1, the effective throughput results of our Monte Carlo simulator are compared with the exact analytical expressions provided in (7) in Section III for different block lengths and delay exponents. Observe that there is a good agreement between the effective throughput given by the theoretical formulas and those obtained by Monte Carlo simulations. As expected, it can be seen that the effective throughput is consistently reduced upon increasing θ and T. For example, when T increases from 1 to 7, the effective throughput reduces from 0.12 to 0.07 bits/s/Hz at $\theta = 6$. Additionally, it is interesting to note that as T increases, the gap between the corresponding curves increases, which implies that its effect becomes more pronounced. These observations explicitly quantify the well-understood physical relationship between the effective throughput and the affordable transmission delay and are consistent with the results presented in [11], [9], and [8].

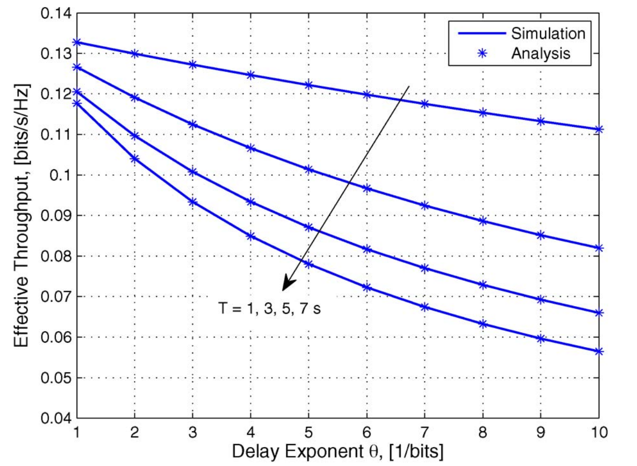

Fig. 1. Simulated and analytical effective throughput against delay exponent θ and T for MISO i.i.d. κ–μ fading channels ($N_t = 2$, $\rho = -10$ dB, $\Omega = 1$, $\kappa = 1$, and $\mu = 1$).

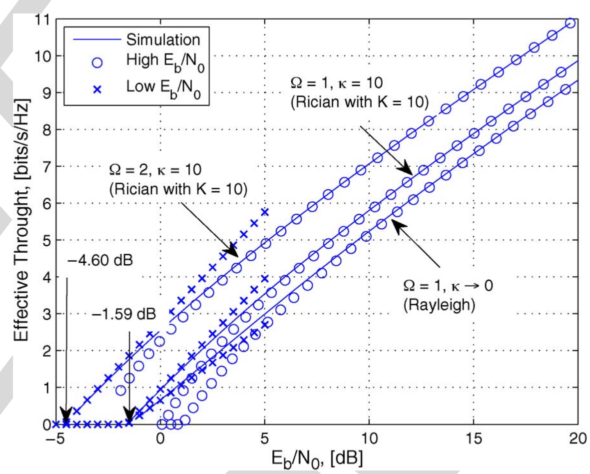

Fig. 2. Simulated high- and low-E_b/N_0 approximation effective throughput against E_b/N_0 for MISO i.i.d. κ–μ fading channels ($N_t = 4$, $T = 1$ s, $\theta = 0.1$, and $\mu = 1$).

Fig. 2 shows the simulated effective throughput, its low-E_b/N_0 approximation seen in (13), and its high-E_b/N_0 approximation quantified in (11) after using the relationship $E_b/N_0 = \rho/R$. Quantitatively, we have a 3-dB reduction in the minimum energy per bit upon increasing the average fading power Ω by 50%. It is also readily shown in Fig. 2 that increasing κ increases the effective throughput due to having an increased throughput versus SNR slope S_0 and so does the average fading power Ω but leaves the required $E_b/N_{0\min}$ value unaffected. The curves shown in Fig. 2 also show that the approximation of the exact throughput is remarkably tight for all the

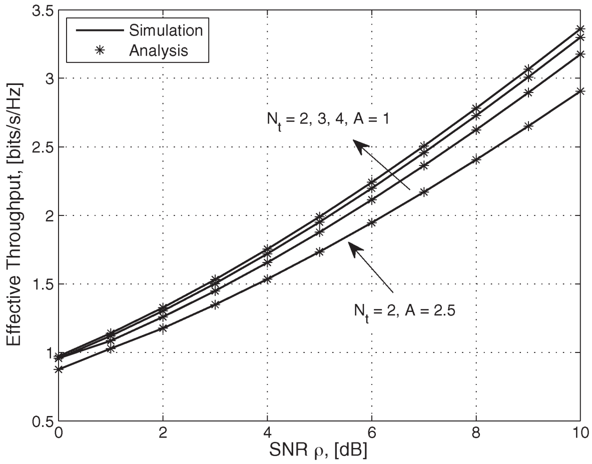

Fig. 3. Simulated and analytical effective throughput against parameters A and N_t for MISO i.n.i.d. κ–μ fading channels [$\Omega = 1$, $\kappa = (2.5, 3.5, 1.1, 1.75)$, and $\mu = (1.5, 0.75, 2.5, 3.75)$].

scenarios considered, but its accuracy is even improved for larger values of the fading parameters.

The simulated and analytical effective throughput of MISO i.n.i.d. κ–μ fading channels recorded for different values of N_t and A as a function of the average SNR ρ are plotted in Fig. 3. The fading parameters are selected as $\kappa = (2.5, 3.5, 1.1, 1.75)$ and $\mu = (1.5, 0.75, 2.5, 3.75)$, respectively. It is clear that the effective throughput is a monotonically decreasing function of A, which implies that improving delay constraints reduces the effective throughput. Additionally, more transmit antennas N_t yield a higher throughput; although, the gap between the corresponding curves decreases as N_t increases. This observation implies that the effect of N_t becomes less pronounced.

VI. Conclusion

The novelty of using the effective throughput as a performance metric is that it quantifies the effects of delay on the attainable throughput, which is reduced upon tightening the affordable delay. As the delay tends to infinity, the effective throughput tends to the ergodic capacity. We have derived new analytical expressions for the exact effective throughput of MISO systems communicating over κ–μ fading channels. Although the exact expression is given in terms of an infinite series, the associated truncation error was also analytically quantified. Quantitatively, it can be seen that as few as ten terms are required for a high accuracy of 10^{-6} in the series. To gain physical insights into the impact of system parameters, we presented a closed-form expression for the effective throughput at high SNRs. Moreover, tractable expressions have been derived for both the minimum transmit energy per information bit required for reliably conveying any nonzero throughput at low SNRs. The results are applicable to the design of next-generation wireless systems.

References

[1] E. Telatar, "Capacity of multi-antenna Gaussian channels," *Eur. Trans. Telecommun.*, vol. 10, no. 6, pp. 585–595, Nov./Dec. 1999.

[2] J. Foschini and J. Gans, "On limits of wireless communications in a fading environment when using multiple antennas," *Wireless Pers. Commun.*, vol. 6, no. 3, pp. 311–335, Mar. 1998.

[3] L. Hanzo, M. El-Hajjar, and O. Alamri, "Near-capacity wireless transceivers and cooperative communications in the MIMO era: Evolution of standards, waveform design, and future perspectives," *Proc. IEEE*, vol. 99, no. 8, pp. 1343–1385, Aug. 2011.

[4] V. Hanly and C. Tse, "Multiaccess fading channels—Part II: Delay-limited capacities," *IEEE Trans. Inf. Theory*, vol. 44, no. 7, pp. 2816–2831, Nov. 1998.

[5] D. Wu and R. Negi, "Effective capacity: A wireless link model for support of quality of service," *IEEE Trans. Wireless Commun.*, vol. 2, no. 4, pp. 630–643, Jul. 2003.

[6] G. Femenias, J. Ramis, and L. Carrasco, "Using two-dimensional Markov models and the effective-capacity approach for cross-layer design in AMC/ARQ-based wireless networks," *IEEE Trans. Veh. Technol.*, vol. 58, no. 8, pp. 4193–4203, Oct. 2009.

[7] S.-W. Ahn, H. Wang, and D. Hong, "Throughput–delay tradeoff of proportional fair scheduling in OFDMA systems," *IEEE Trans. Veh. Technol.*, vol. 60, no. 9, pp. 4620–4626, Nov. 2011.

[8] A. Jorswieck, R. Mochaourab, and M. Mittelbach, "Effective capacity maximization in multi-antenna channels with covariance feedback," *IEEE Trans. Wireless Commun.*, vol. 9, no. 10, pp. 2988–2993, Oct. 2010.

[9] C. Zhong, T. Ratnarajah, K. Wong, and S. Alouini, "Effective capacity of correlated MISO channels," in *Proc. IEEE ICC*, Kyoto, Japan, Jun. 2011, pp. 1–5.

[10] D. Li, "Effect of channel estimation errors on arbitrary transmit antenna selection for cognitive MISO systems," *IEEE Commun. Lett.*, vol. 15, no. 6, pp. 656–658, Jun. 2011.

[11] M. Matthaiou, G. Alexandropoulos, H. Ngo, and E. Larsson, "Analytic framework for the effective rate of MISO fading channels," *IEEE Trans. Commun.*, vol. 60, no. 6, pp. 1741–1751, Jun. 2012.

[12] D. Yacoub, "The κ–μ distribution and the η–μ distribution," *IEEE Antennas Propag. Mag.*, vol. 49, no. 1, pp. 68–81, Feb. 2007.

[13] L. Liu and J.-F. Chamberland, "On the effective capacities of multiple-antenna Gaussian channels," in *Proc. IEEE Int. Symp. Inf. Theory*, Toronto, ON, Canada, Jul. 2008, pp. 2583–2587.

[14] S. Gradshteyn and M. Ryzhik, *Table of Integrals, Series, and Products.*, 7th ed. San Diego, CA, USA: Academic, 2007.

[15] M. Kang and S. Alouini, "Capacity of MIMO Rician channels," *IEEE Trans. Wireless Commun.*, vol. 5, no. 1, pp. 112–122, Jan. 2006.

[16] Wolfram, *The wolfram functions site*. [Online]. Available: http://functions.wolfram.com

[17] M. Abramowitz and A. Stegun, *Handbook of Mathematical Functions with Formulas, Graphs, and Mathematical Tables*, 9th ed. New York, NY, USA: Dover, 1964.

[18] P. Prudnikov, A. Brychkov, and I. Marichev, *Integrals and Series, Volume 4: Direct Laplace Transforms*. New York, NY, USA: Gordon and Breach, 1992.

[19] C. Gursoy, "MIMO wireless communications under statistical queueing constraints," *IEEE Trans. Inf. Theory*, vol. 57, no. 9, pp. 5897–5917, Sep. 2011.

[20] A. Lozano, M. Tulino, and S. Verdú, "Multiple-antenna capacity in the low-power regime," *IEEE Trans. Inf. Theory*, vol. 49, no. 10, pp. 2527–2544, Oct. 2003.

[21] P. Peppas, "Sum of nonidentical squared κ– μ variates and applications in the performance analysis of diversity receivers," *IEEE Trans. Veh. Technol.*, vol. 61, no. 1, pp. 413–419, Jan. 2012.

[22] A. Castaño-Martıacute;nez and F. López-Blázquez, "Distribution of a sum of weighted noncentral chi-square variables," *Test*, vol. 14, no. 2, pp. 397–415, Dec. 2005.

AUTHOR QUERY

NO QUERY.

Correspondence

The Effective Throughput of MISO Systems Over κ–μ Fading Channels

Jiayi Zhang, *Student Member, IEEE*, Zhenhui Tan, Haibo Wang, Qing Huang, and Lajos Hanzo, *Fellow, IEEE*

***Abstract*—The *effective throughput* of multiple-input–single-output (MISO) systems communicating over both independent and identically distributed (i.i.d.) and independent and nonidentically distributed (i.n.i.d.) κ–μ fading channels is investigated under delay constraints. New analytical expressions are derived for the exact effective throughput of both channels. Moreover, we present tractable closed-form effective throughput expressions in the asymptotically high- and low-signal-to-noise-ratio (SNR) regimes for i.i.d. κ–μ fading channels. These results enable us to investigate the impact of system parameters on the effective throughput of MISO κ–μ fading channels. We demonstrate that as the affordable delay tends to infinity, the effective throughput is increased to the classic ergodic capacity. By contrast, the effective throughput of delay-constrained near-real-time systems fails to approach the ergodic capacity.**

***Index Terms*—Delay constraint, delay-limited capacity, effective capacity, κ–μ distribution, multiple-input single-output (MISO).**

I. Introduction

The ergodic capacity of multiple-antenna systems has been investigated for transmission over various fading channels in [1]–[3]. However, emerging real-time applications, such as voice over Internet Protocol and mobile TV, have imposed stringent quality-of-service (QoS) constraints. **In this context, Shannon's ergodic capacity cannot account for the transmission delay of the system. However, it would be highly desirable to quantify the delay-limited capacity of a system, which is a challenging task. The first contribution in this content was produced by Hanly and Tse in** [4]. Hence, a QoS metric capable of capturing the delay constraints of communication systems is required. Motivated by this open problem, the concept of effective throughput (or effective capacity, effective rate) has been proposed in [5] for taking the system's delay into account. Since then, several authors have investigated the effective capacity of various systems. For example, Femenias *et al.* in [6] investigated the effective capacity of wireless cross-layer networks combining adaptive modulation and coding at the physical layer with an automatic repeat request protocol at the data-link layer. In [7], an analytical model of the effective capacity found in proportional fair scheduling used in orthogonal frequency-division multiple-access systems in the context of user multiplexing was presented.

The effective throughput of multiple-input–single-output (MISO) systems, such as the optimal precoding scheme relying on covariance feedback, was derived for correlated MISO systems [8], whereas that of correlated MISO channels was presented in [9]. In [10], Li characterized the effective throughput of cognitive MISO systems subjected to channel estimation errors. Moreover, Matthaiou *et al.* in [11] provided a detailed effective throughput analysis of Nakagami-m, Rician, and generalized-K MISO fading channels. However, the existence of these well-known fading distributions is based on the assumption of a homogeneous scattering environment, which is often unrealistic, since the waves reflected by a surface are spatially correlated in most propagation environments.

Hence, the κ–μ distribution has been proposed in [12] for characterizing the inhomogeneous nature of fading channels. This generalized fading model is capable of providing a better fit to experimental data than the aforementioned models. Additionally, it has been shown in [12] that the κ–μ distribution encompasses the Rician, Nakagami-m, and Rayleigh distributions as special cases. *Against this background, we solve the open problem of providing both exact and asymptotic high-signal-to-noise-ratio (SNR) and low-SNR expressions for the effective throughput of independent and identically distributed (i.i.d.) and independent and nonidentically distributed (i.n.i.d.) κ–μ fading channels.*

The rest of this paper is organized as follows. Section II describes the general system model and the mathematical characteristics of κ–μ fading channels. In Section III, we derive new exact expressions for the effective throughput of MISO systems communicating over i.i.d. κ–μ fading channels and present closed-form effective throughput expressions both for high SNRs and for the minimum transmit energy per information bit for the sake of quantifying the effect of system parameters on the effective throughput. Moreover, the effective throughput for the case of i.n.i.d. κ–μ fading channels is analyzed in Section IV. Finally, our theoretical and Monte Carlo simulation results are compared in Section V in terms of the effective throughput, and Section VI concludes this paper.

II. System and Channel Model

We consider a MISO system model and assume that the transmitter is equipped with N_t antennas. The flat-fading channel's input–output relation can be expressed as $y = \mathbf{h}\mathbf{x} + n$, where $\mathbf{h} \in \mathbb{C}^{1\times N_t}$ denotes the MISO channel's fading vector, whereas $\mathbf{x}$ is the transmit vector having a covariance of $\mathtt{E}\{\mathbf{x}\mathbf{x}^\dagger\} = \mathbf{Q}$, where $\mathtt{E}\{\cdot\}$ is the expectation operator, which is subjected to the sum-power constraint of $\mathrm{tr}(\mathbf{Q}) \le P$, where $\mathrm{tr}(\cdot)$ is the matrix trace. Moreover, n represents the complex additive white Gaussian noise term with zero mean and variance N_0, respectively. Finally, we assume that the same power is assigned to the transmit antennas; hence, we have $\mathbf{Q} = (P/N_t)\mathbf{I}$.

As a generalized link-level capacity notion of uncorrelated stationary fading channels, whose response varies from one transmission block to another by obeying a certain distribution but remains constant

Manuscript received January 2, 2013; revised August 5, 2013; accepted August 6, 2013. This work was supported in part by the National Natural Science Foundation of China under Grant 61071075 and Grant 61001071, by the National ST Major Project under Grant 2011ZX03005-004-03, and by the Fundamental Research Funds for the Central Universities under Grant 2012JBM018. The review of this paper was coordinated by Prof. M. Daoud.

J. Zhang is with the Institute of Broadband Wireless Mobile Communications and the State Key Laboratory of Rail Traffic Control and Safety, Beijing Jiaotong University, Beijing 100044, China (e-mail: jayizhang@bjtu.edu.cn).

Z. Tan, H. Wang, and Q. Huang are with the Institute of Broadband Wireless Mobile Communications, Beijing Jiaotong University, Beijing 100044, China (e-mail: zhhtan@bjtu.edu.cn; hbwang@bjtu.edu.cn; qhuang1@bjtu.edu.cn).

L. Hanzo is with the School of Electrical and Computer Science, University of Southampton, Southampton SO17 1BJ, U.K. (e-mail: lh@ecs.soton.ac.uk).

Color versions of one or more of the figures in this paper are available online at http://ieeexplore.ieee.org.

Digital Object Identifier 10.1109/TVT.2013.2277992

within a single block, the effective capacity of the service process is defined as [13][1]

$$\alpha(\theta) = -(1/\theta T)\ \ln\left(\mathtt{E}\left\{\exp(-\theta T C)\right\}\right), \qquad \theta \neq 0 \tag{1}$$

where C represents the system's throughput during a single block, and T denotes the duration of the block, whereas the delay exponent

$$\theta = -\lim_{l_{\text{th}}\to\infty} \frac{\ln \Pr[L > l_{\text{th}}]}{l_{\text{th}}} \tag{2}$$

of (1) reflects that any throughput improvement attained at the cost of a high delay is devalued. In (2), l_{th} is the threshold of queue length, and L is the equilibrium queue length of the buffer assumed to be available at the transmitter. When $l_{\text{th}} \to \infty$, the tail distribution function $\Pr[L > l_{\text{th}}]$ can be asymptotically written as $\Pr[L > l_{\text{th}}] \approx e^{\theta l_{\text{th}}}$ according to the large deviations theory [5]. Again, the delay exponent has to satisfy the constraint of $\theta \geq \theta_0$, where θ_0 is the minimum required decay rate. Once a delay requirement is violated, the corresponding data packet is discarded in the queue. More particularly, a larger θ_0 implies a tighter delay constraint. Note that when no delay constraint is imposed, i.e., we have $\theta_0 \to 0$, the effective throughput tends to the classic ergodic throughput of the corresponding wireless channel.

Assuming that the transmitter sends uncorrelated circularly symmetric zero-mean complex Gaussian signals, the effective throughput can be succinctly expressed as follows [11]:

$$R(\rho,\theta) = -\frac{1}{A}\log_2\left(\mathtt{E}\left\{\left(1+\frac{\rho}{N_t}\mathbf{h}\mathbf{h}^{\dagger}\right)^{-A}\right\}\right)\ \text{bits/s/Hz} \tag{3}$$

where we have $A = \theta T B/\ln 2$, with B denoting the bandwidth of the system, whereas ρ is the average SNR.

The κ–μ distribution models the small-scale variation of the fading signal in a nonhomogeneous environment. The probability density function (pdf) of the κ–μ fading channels' output SNR is given by [12, eq. (10)]

$$p_{\kappa-\mu}(\omega) = \frac{\mu(1+\kappa)^{\frac{\mu+1}{2}}\omega^{\frac{\mu-1}{2}}}{\exp(\mu\kappa)\kappa^{\frac{\mu-1}{2}}\Omega^{\frac{\mu+1}{2}}}\exp\left(-\frac{\mu(1+\kappa)\omega}{\Omega}\right) \times I_{\mu-1}\left(2\mu\sqrt{\frac{\kappa(1+\kappa)\,\omega}{\Omega}}\right) \tag{4}$$

where κ denotes the ratio between the total power of the dominant components and the total power of the scattered waves, μ is related to the number of multipath clusters, and $I_v(\cdot)$ is the modified Bessel function of the first kind with order v [14, eq. (8.445)].

III. Independent and Identical κ–μ Fading

A. Exact Analysis

Here, we present the exact effective throughput analysis of the κ–μ fading models introduced in Section II. More specifically, the entries of channel vector $\mathbf{h}$ are assumed to be i.i.d. κ–μ random variables (RVs).

We commence our analysis by invoking [12], where it was shown that the sum of M i.i.d. squared κ–μ distributed RVs with parameters κ, μ, and Ω is also a κ–μ distribution with parameters κ, $M\mu$, and $M\Omega$. Using [12, eq. (10)], after a number of manipulations, we arrive at the pdf of $z = \sum_{k=1}^{N_t}|h_k|^2$, i.e.,

$$p_{\text{i.i.d.}}(z) = \frac{\mu N_t(1+\kappa)^{\frac{\mu N_t+1}{2}} z^{\frac{\mu N_t-1}{2}}}{e^{\mu N_t\kappa}\kappa^{\frac{\mu N_t-1}{2}}(\Omega N_t)^{\frac{\mu N_t+1}{2}}}\exp\left(-\frac{\mu(1+\kappa)z}{\Omega}\right) \times I_{\mu N_t-1}\left(2u\sqrt{\frac{\kappa(1+\kappa)N_t z}{\Omega}}\right) \tag{5}$$

$$= \frac{\mu N_t(1+\kappa)^{\frac{\mu N_t+1}{2}} z^{\frac{\mu N_t-1}{2}}}{e^{\mu N_t\kappa}\kappa^{\frac{\mu N_t-1}{2}}(\Omega N_t)^{\frac{\mu N_t+1}{2}}}\exp\left(-\frac{\mu(1+\kappa)z}{\Omega}\right) \times \sum_{l=0}^{\infty}\frac{1}{l!\Gamma(\mu N_t+l)}\left(\mu\sqrt{\frac{\kappa(1+\kappa)N_t z}{\Omega}}\right)^{\mu N_t+2l-1} \tag{6}$$

where we proceed from (5) to (6) by exploiting [14, eq. (8.445)]. Upon substituting (6) into (3), there is an integral in the form of $(1+\rho z/N_t)^{-A}$, $z^{\mu N_t+l-1}$, and $\exp(-(\mu(1+\kappa)z/\Omega))$. The effective throughput of MISO i.i.d. κ–μ fading channels is given by

$$R_{\text{i.i.d.}}(\rho,\theta) = \frac{\mu N_t\kappa}{A\ln 2} + \log_2\left(\frac{\Omega\rho}{\mu N_t(1+\kappa)}\right) - \frac{1}{A}\log_2\left(\sum_{l=0}^{\infty}\frac{(\mu N_t\kappa)^l}{\Gamma(l+1)}U\left(A; A+1-\mu N_t-l; \frac{\mu N_t(1+\kappa)}{\Omega\rho}\right)\right) \tag{7}$$

where $U(\cdot)$ is the Tricomi hypergeometric function [14, eq. (13.1.3)], and we have used the integral equation of [15, eq. (39)], i.e.,

$$\int_0^{\infty}(1+ax)^{-v}x^{q-1}e^{-px}dx = a^{-q}\Gamma(q)U\left(q, q+1-v, p/a\right)$$

where the conditions of $\mathrm{Re}(q) > 0$, $\mathrm{Re}(p) > 0$, and $\mathrm{Re}(a) > 0$ are met. In addition, Kummer's transformation $U(a; b; x) = x^{1-b}U(a-b+1; 2-b; x)$ [16, eq. (07.33.17.0007.01)] is used. Note that for the case of Rician fading channels (e.g., $\kappa = K$, $\mu = 1$, where K is the Rician K-factor), (7) reduces to [11, eq. (34)].

Since (7) is expressed in the form of an infinite series, we should demonstrate its convergence by seeking to quantify the truncation error imposed by a limited number of terms. Assuming that T_0 terms are used, the associated truncation error E_0 can be expressed as

$$E_0 = \sum_{l=T_0}^{\infty}\frac{(\mu N_t\kappa)^l}{\Gamma(l+1)}U\left(A; A+1-\mu N_t-l; \frac{\mu N_t(1+\kappa)}{\Omega\rho}\right) < U\left(A; A+1-\mu N_t-T_0; \frac{\mu N_t(1+\kappa)}{\Omega\rho}\right)\sum_{l=T_0}^{\infty}\frac{(\mu N_t\kappa)^l}{\Gamma(l+1)} \tag{8}$$

where we have exploited the fact that $U(a, b-l, z)$ is a monotonically decreasing function of l. With the aid of [17, eq. (6.5.4)] and [17, eq. (6.5.29)], (8) may be streamlined to

$$E_0 < U\left(A; A+1-\mu N_t-T_0; \frac{\mu N_t(1+\kappa)}{\Omega\rho}\right) \times \exp\left(\mu\kappa N_t\right)\left(1-\frac{\Gamma(T_0,\mu\kappa N_t)}{\Gamma(T_0)}\right) \tag{9}$$

where $\Gamma(\cdot,\cdot)$ represents the upper incomplete gamma function [14, eq. (8.350.2)].

[1]The packet arrival process and the server strategy employed in the queuing system are those introduced in [5] and [13].

The given expressions are exact; however, they only provide limited physical insights into the quantitative effects of the parameters (e.g., the number of transmit antennas, the delay-related exponent, and the number of multipath clusters) on the effective throughput. Let us hence elaborate further by considering both the high- and low-SNR regions of operation.

B. Asymptotic Analysis

We commence with the high-SNR analysis. By retaining only the dominant term in (3) as $\rho \to \infty$, we arrive at

$$\mathtt{E}\left\{\left(\frac{\rho}{N_t}\mathbf{h}\mathbf{h}^\dagger\right)^{-A}\right\} = \left(\frac{\rho}{N_t}\right)^{-A} \frac{\mu N_t (1+\kappa)^{\frac{\mu N_t+1}{2}}}{e^{\mu N_t \kappa}\kappa^{\frac{\mu N_t-1}{2}}(\Omega N_t)^{\frac{\mu N_t+1}{2}}} \times \int_0^\infty \frac{z^{(\mu N_t-1)/2-A}}{\exp\left(\mu(1+\kappa)\,z/\Omega\right)} I_{\mu N_t-1}\left(2\mu\sqrt{\frac{\kappa(1+\kappa)\,N_t z}{\Omega}}\right) dz. \tag{10}$$

The given integral can now be evaluated using [18, eq. (3.15.2.5)], upon exploiting that $A < \mu N_t$. Finally, the effective throughput attained at high SNRs and for $A < \mu N_t$ may be approximated for MISO κ–μ fading channels as

$$R^{\infty}_{\mathrm{i.i.d.}}(\rho,\theta) = \log_2\left(\frac{\Omega\rho}{\mu N_t(1+\kappa)}\right) + \frac{\kappa\mu N_t}{A\ln 2} - \frac{1}{A}\log_2\left(\frac{\Gamma(\mu N_t - A)}{\Gamma(\mu N_t)}\,{}_1F_1(\mu N_t - A;\mu N_t;\kappa\mu N_t)\right) \tag{11}$$

where ${}_1F_1$ is the confluent hypergeometric function [14, eq. (9.238.2)]. Note that the effective throughput achieved at high SNRs is a monotonically increasing function of κ. This is anticipated, since larger values of κ result in more deterministic fading. When considering the Rician fading case, (11) reduces to [11, eq. (49)].

Let us now investigate the effective throughput of κ–μ fading channels in the power-limited low-SNR region, where the effective throughput can be approximated by a second-order Taylor expansion of the SNR following the generic methodology in [19]. More particularly, we can approximate the effective throughput as $\rho \to 0^+$ according to

$$R(\rho,\theta) = R'(0,\theta)\,\rho + R''(0,\theta)\frac{\rho^2}{2} + o\left(\rho^2\right) \tag{12}$$

where $R'(0,\theta)$ and $R''(0,\theta)$ denote the first- and second-order derivatives of the effective throughput with respect to the SNR, ρ, at $\rho = 0$, respectively.

However, it has been shown in [20] that the Taylor expansion method may, in fact, result in misleading conclusions regarding the impact of the channel in the low-SNR region. Hence, it is beneficial to explore the effective throughput at low SNRs in terms of the normalized transmit energy per information bit E_b/N_0, which is formulated as [20]

$$R\left(\frac{E_b}{N_0}\right) \approx S_0 \log_2\left(\frac{E_b}{N_0}\Big/\frac{E_b}{N_0}_{\min}\right) \tag{13}$$

where $E_b/N_{0\,\min}$ is the minimum normalized energy per information bit required for reliably conveying any nonzero throughput, whereas S_0 denotes the throughput versus SNR slope defined in [8]. These metrics are defined respectively as

$$\frac{E_b}{N_0}_{\min} \triangleq \lim_{\rho\to 0}\frac{\rho}{R(\rho,\theta)} = \frac{1}{R'(0,\theta)} \tag{14}$$

$$S_0 \triangleq -\frac{2\left[R'(0,\theta)\right]^2 \ln 2}{R''(0,\theta)}. \tag{15}$$

Due to space limitations, we omit the explicit details, and upon following a similar line of reasoning as in [9, Appendix I], we arrive at the first- and second-order derivatives seen in (14) and (15) in the form of

$$R'(0,\theta) = \frac{1}{N_t \ln 2}\mathtt{E}\{\mathbf{h}\mathbf{h}^\dagger\} \tag{16}$$

$$R''(0,\theta) = \frac{A}{N_t^2 \ln 2}\left(\mathtt{E}\{\mathbf{h}\mathbf{h}^\dagger\}\right)^2 - \frac{A+1}{N_t^2\ln 2}E\left\{(\mathbf{h}\mathbf{h}^\dagger)^2\right\}. \tag{17}$$

Recalling that $\mathtt{E}\{|h_k|^2\} = \Omega$, we may readily infer that $\mathtt{E}\{\mathbf{h}\mathbf{h}^\dagger\} = N_t\Omega$. With the aid of (4) and [18, eq. (3.15.2.5)], the fourth moment of $|h_k|$ can now be expressed as

$$\mathtt{E}\left\{|h_k|^4\right\} = N_t\Omega^2\left(\frac{1+2\kappa}{\mu(1+\kappa)^2} + N_t\right) \tag{18}$$

where we have utilized [14, eq. (9.212.1)] and [14, eq. (9.210.1)]. With (18) at our disposal, we can readily deduce that

$$\begin{aligned}\mathtt{E}\left\{(\mathbf{h}\mathbf{h}^\dagger)^2\right\} &= \mathtt{E}\left\{\left(\sum_{k=1}^{N_t}|h_k|^2\right)^2\right\}\\ &= \sum_{k=1}^{N_t}\mathtt{E}\left\{|h_k|^4\right\} + \sum_{k=1}^{N_t}\sum_{j=1,j\neq k}^{N_t}\mathtt{E}\left\{|h_k|^2|h_j|^2\right\}\\ &= N_t\Omega^2\left(\frac{1+2\kappa}{\mu(1+\kappa)^2} + N_t\right).\end{aligned} \tag{19}$$

Substituting (19) into (17) and then applying (14) and (15), the low-SNR metrics of MISO κ–μ fading channels can be respectively expressed as

$$\frac{E_b}{N_0}_{\min} = \frac{\ln 2}{\Omega} \tag{20}$$

$$S_0 = \frac{2\mu N_t(1+\kappa)^2}{(A+1)(1+2\kappa) + \mu N_t(1+\kappa)^2}. \tag{21}$$

Observe in (21) that the low-SNR slope is an increasing function of both κ and μ, whereas it is a monotonically decreasing function of A, satisfying $0 < S_0 < 2$ for a fixed N_t. It is also worth mentioning that $E_b/N_{0\,\min}$ is independent of both κ and delay constraint θ. Note that for the case of Rician fading channels, the throughput-versus-SNR-slope expression of (21) reduces to

$$S_0 = \frac{2N_t(K+1)^2}{N_t(K+1)^2 + (A+1)^{2K+1}} \tag{22}$$

which coincides with [11, eq. (41)].

IV. Independent and Nonidentical κ–μ Fading

Let us now move on to consider the case of wireless systems communicating over i.n.i.d. MISO κ–μ fading channels. The pdf of the sum of M i.n.i.d. squared κ–μ distributed RVs associated with parameters κ_m, μ_m, and Ω_m is given by [21, eq. (4)], i.e.,

$$p_{\text{i.n.i.d.}}(z) = \frac{e^{-\frac{z}{2\beta}} z^{V-1}}{(2\beta)^V \Gamma(V)} \sum_{k=0}^{\infty} \frac{k! c_k}{(V)_k} L_k^{(V-1)} \left(\frac{Uz}{2\beta\xi} \right) \tag{23}$$

where $V = \sum_{m=1}^{M} \mu_m$, $(u)_v = \Gamma(u+v)/\Gamma(u)$ is the Pochhammer symbol [14], and $L_n^{\alpha}(\cdot)$ is the generalized Laguerre polynomial [16, eq. (05.08.02.0001.01)], namely

$$L_n^v(y) = \frac{\Gamma(v+n+1)}{n!} \sum_{q=0}^{n} \frac{(-n)_q y^q}{q! \Gamma(v+q+1)}, \; n \in \mathbb{N}. \tag{24}$$

Then, (23) can be alternatively expressed as

$$p_{\text{i.n.i.d.}}(z) = \frac{e^{\frac{-z}{2\beta}}}{(2\beta)^V} \sum_{k=0}^{\infty} c_k \sum_{q=0}^{k} \frac{(-k)_q z^{q+V-1}}{q! \Gamma(V+q)} \left(\frac{V}{2\beta\xi} \right)^q. \tag{25}$$

Note that the coefficients c_k can be recursively obtained following the equations [21, eq. (5a–5c)]

$$c_k = \frac{1}{k} \sum_{j=0}^{k} c_j d_{k-j}, \qquad k \geqslant 1 \tag{26}$$

$$c_0 = \left(\frac{V}{\xi} \right)^V \exp\left(-\frac{1}{2} \sum_{m=1}^{M} \frac{\lambda_m a_m (V-\xi)}{\beta\xi + a_m(V-\xi)} \right) \times \prod_{m=1}^{M} \left(1 + \frac{a_m}{\beta}(V/\xi - 1) \right)^{-\mu_m} \tag{27}$$

$$d_j = -\frac{j\beta V}{2\xi} \sum_{m=1}^{M} \lambda_m a_m (\beta - a_m)^{j-1} \left(\frac{\xi}{\beta\xi + a_m(V-\xi)} \right)^{j+1} + \sum_{m=1}^{M} \mu_m \left(\frac{1 - a_m/\beta}{1 + (a_m/\beta)(V/\xi - 1)} \right)^j, \qquad j \geqslant 1 \tag{28}$$

where $\lambda_m = 2\mu_m\kappa_m$, $a_m = \Omega_m / 2\mu_m(1+\kappa_m)$. Note that parameters ξ and β are chosen to guarantee the uniform convergence of (23) according to [22, Remark 3.1]. By substituting (25) into (3) and using the identity [15, eq. (39)], we arrive at the effective throughput expression of MISO i.n.i.d. κ–μ fading channels formulated as

$$R_{\text{i.n.i.d.}} = \log_2\left(\frac{2\beta\rho}{N_t} \right) - \frac{1}{A} \sum_{k=0}^{\infty} c_k \sum_{q=0}^{k} \frac{(-k)_q}{q!} \left(\frac{V}{\xi} \right)^q \times U\left(A; A+1-q-V; \frac{N_t}{2\beta\rho} \right). \tag{29}$$

V. Numerical Results

Here, the theoretical analysis presented in Sections III and IV is validated with the aid of Monte Carlo simulations, which were derived by averaging the results over 10^7 independent κ–μ channel realizations. We generate the squared κ–μ fading samples using the noncentral chi-square distribution method in [21]. These results are provided for characterizing the effects of different system and channel parameters on the effective throughput of MISO systems communicating over κ–μ fading channels. Without loss of generality, we normalize the bandwidth of the system as $B = 1$ Hz.

In Fig. 1, the effective throughput results of our Monte Carlo simulator are compared with the exact analytical expressions provided in (7) in Section III for different block lengths and delay exponents. Observe that there is a good agreement between the effective throughput given by the theoretical formulas and those obtained by Monte Carlo simulations. As expected, it can be seen that the effective throughput is consistently reduced upon increasing θ and T. For example, when T increases from 1 to 7, the effective throughput reduces from 0.12 to 0.07 bits/s/Hz at $\theta = 6$. Additionally, it is interesting to note that as T increases, the gap between the corresponding curves increases, which implies that its effect becomes more pronounced. These observations explicitly quantify the well-understood physical relationship between the effective throughput and the affordable transmission delay and are consistent with the results presented in [11], [9], and [8].

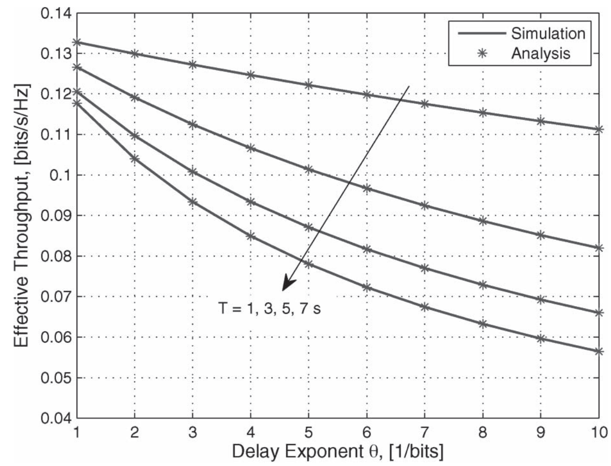

Fig. 1. Simulated and analytical effective throughput against delay exponent θ and T for MISO i.i.d. κ–μ fading channels ($N_t = 2$, $\rho = -10$ dB, $\Omega = 1$, $\kappa = 1$, and $\mu = 1$).

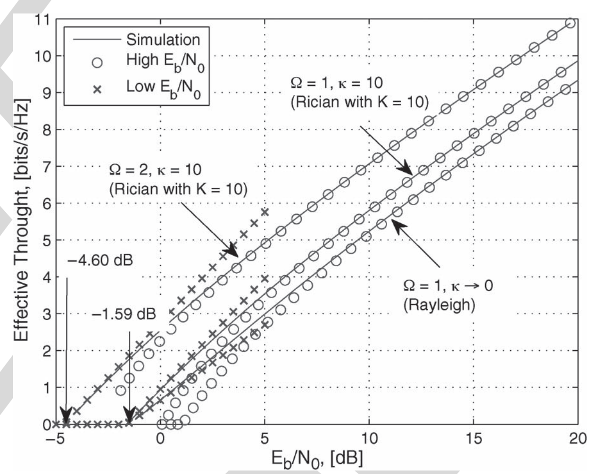

Fig. 2. Simulated high- and low-E_b/N_0 approximation effective throughput against E_b/N_0 for MISO i.i.d. κ–μ fading channels ($N_t = 4$, $T = 1$ s, $\theta = 0.1$, and $\mu = 1$).

Fig. 2 shows the simulated effective throughput, its low-E_b/N_0 approximation seen in (13), and its high-E_b/N_0 approximation quantified in (11) after using the relationship $E_b/N_0 = \rho/R$. Quantitatively, we have a 3-dB reduction in the minimum energy per bit upon increasing the average fading power Ω by 50%. It is also readily shown in Fig. 2 that increasing κ increases the effective throughput due to having an increased throughput versus SNR slope S_0 and so does the average fading power Ω but leaves the required $E_b/N_{0_{\min}}$ value unaffected. The curves shown in Fig. 2 also show that the approximation of the exact throughput is remarkably tight for all the

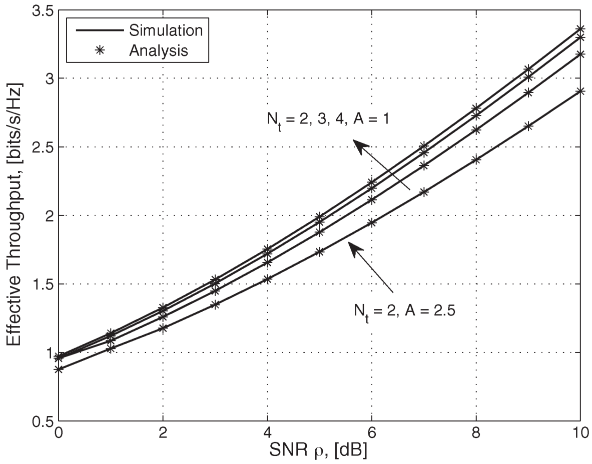

Fig. 3. Simulated and analytical effective throughput against parameters A and N_t for MISO i.n.i.d. κ–μ fading channels [$\Omega = 1$, $\kappa = (2.5, 3.5, 1.1, 1.75)$, and $\mu = (1.5, 0.75, 2.5, 3.75)$].

scenarios considered, but its accuracy is even improved for larger values of the fading parameters.

The simulated and analytical effective throughput of MISO i.n.i.d. κ–μ fading channels recorded for different values of N_t and A as a function of the average SNR ρ are plotted in Fig. 3. The fading parameters are selected as $\kappa = (2.5, 3.5, 1.1, 1.75)$ and $\mu = (1.5, 0.75, 2.5, 3.75)$, respectively. It is clear that the effective throughput is a monotonically decreasing function of A, which implies that improving delay constraints reduces the effective throughput. Additionally, more transmit antennas N_t yield a higher throughput; although, the gap between the corresponding curves decreases as N_t increases. This observation implies that the effect of N_t becomes less pronounced.

VI. Conclusion

The novelty of using the effective throughput as a performance metric is that it quantifies the effects of delay on the attainable throughput, which is reduced upon tightening the affordable delay. As the delay tends to infinity, the effective throughput tends to the ergodic capacity. We have derived new analytical expressions for the exact effective throughput of MISO systems communicating over κ–μ fading channels. Although the exact expression is given in terms of an infinite series, the associated truncation error was also analytically quantified. Quantitatively, it can be seen that as few as ten terms are required for a high accuracy of 10^{-6} in the series. To gain physical insights into the impact of system parameters, we presented a closed-form expression for the effective throughput at high SNRs. Moreover, tractable expressions have been derived for both the minimum transmit energy per information bit required for reliably conveying any nonzero throughput at low SNRs. The results are applicable to the design of next-generation wireless systems.

References

[1] E. Telatar, "Capacity of multi-antenna Gaussian channels," *Eur. Trans. Telecommun.*, vol. 10, no. 6, pp. 585–595, Nov./Dec. 1999.

[2] J. Foschini and J. Gans, "On limits of wireless communications in a fading environment when using multiple antennas," *Wireless Pers. Commun.*, vol. 6, no. 3, pp. 311–335, Mar. 1998.

[3] L. Hanzo, M. El-Hajjar, and O. Alamri, "Near-capacity wireless transceivers and cooperative communications in the MIMO era: Evolution of standards, waveform design, and future perspectives," *Proc. IEEE*, vol. 99, no. 8, pp. 1343–1385, Aug. 2011.

[4] V. Hanly and C. Tse, "Multiaccess fading channels—Part II: Delay-limited capacities," *IEEE Trans. Inf. Theory*, vol. 44, no. 7, pp. 2816–2831, Nov. 1998.

[5] D. Wu and R. Negi, "Effective capacity: A wireless link model for support of quality of service," *IEEE Trans. Wireless Commun.*, vol. 2, no. 4, pp. 630–643, Jul. 2003.

[6] G. Femenias, J. Ramis, and L. Carrasco, "Using two-dimensional Markov models and the effective-capacity approach for cross-layer design in AMC/ARQ-based wireless networks," *IEEE Trans. Veh. Technol.*, vol. 58, no. 8, pp. 4193–4203, Oct. 2009.

[7] S.-W. Ahn, H. Wang, and D. Hong, "Throughput–delay tradeoff of proportional fair scheduling in OFDMA systems," *IEEE Trans. Veh. Technol.*, vol. 60, no. 9, pp. 4620–4626, Nov. 2011.

[8] A. Jorswieck, R. Mochaourab, and M. Mittelbach, "Effective capacity maximization in multi-antenna channels with covariance feedback," *IEEE Trans. Wireless Commun.*, vol. 9, no. 10, pp. 2988–2993, Oct. 2010.

[9] C. Zhong, T. Ratnarajah, K. Wong, and S. Alouini, "Effective capacity of correlated MISO channels," in *Proc. IEEE ICC*, Kyoto, Japan, Jun. 2011, pp. 1–5.

[10] D. Li, "Effect of channel estimation errors on arbitrary transmit antenna selection for cognitive MISO systems," *IEEE Commun. Lett.*, vol. 15, no. 6, pp. 656–658, Jun. 2011.

[11] M. Matthaiou, G. Alexandropoulos, H. Ngo, and E. Larsson, "Analytic framework for the effective rate of MISO fading channels," *IEEE Trans. Commun.*, vol. 60, no. 6, pp. 1741–1751, Jun. 2012.

[12] D. Yacoub, "The κ–μ distribution and the η–μ distribution," *IEEE Antennas Propag. Mag.*, vol. 49, no. 1, pp. 68–81, Feb. 2007.

[13] L. Liu and J.-F. Chamberland, "On the effective capacities of multiple-antenna Gaussian channels," in *Proc. IEEE Int. Symp. Inf. Theory*, Toronto, ON, Canada, Jul. 2008, pp. 2583–2587.

[14] S. Gradshteyn and M. Ryzhik, *Table of Integrals, Series, and Products*., 7th ed. San Diego, CA, USA: Academic, 2007.

[15] M. Kang and S. Alouini, "Capacity of MIMO Rician channels," *IEEE Trans. Wireless Commun.*, vol. 5, no. 1, pp. 112–122, Jan. 2006.

[16] Wolfram, *The wolfram functions site*. [Online]. Available: http://functions.wolfram.com

[17] M. Abramowitz and A. Stegun, *Handbook of Mathematical Functions with Formulas, Graphs, and Mathematical Tables*, 9th ed. New York, NY, USA: Dover, 1964.

[18] P. Prudnikov, A. Brychkov, and I. Marichev, *Integrals and Series, Volume 4: Direct Laplace Transforms*. New York, NY, USA: Gordon and Breach, 1992.

[19] C. Gursoy, "MIMO wireless communications under statistical queueing constraints," *IEEE Trans. Inf. Theory*, vol. 57, no. 9, pp. 5897–5917, Sep. 2011.

[20] A. Lozano, M. Tulino, and S. Verdú, "Multiple-antenna capacity in the low-power regime," *IEEE Trans. Inf. Theory*, vol. 49, no. 10, pp. 2527–2544, Oct. 2003.

[21] P. Peppas, "Sum of nonidentical squared κ– μ variates and applications in the performance analysis of diversity receivers," *IEEE Trans. Veh. Technol.*, vol. 61, no. 1, pp. 413–419, Jan. 2012.

[22] A. Castaño-Martıacute;nez and F. López-Blázquez, "Distribution of a sum of weighted noncentral chi-square variables," *Test*, vol. 14, no. 2, pp. 397–415, Dec. 2005.

AUTHOR QUERY

NO QUERY.